Received: 13 March 2023 | Revised: 28 July 2023 | Accepted: 3 August 2023

DOI: 10.1111/pce.14693

ORIGINAL ARTICLE

Plant, Cell & Environment | WILEY

Tissue-specific stilbene accumulation is an early response to wounding/grafting as revealed by using spatial and temporal metabolomics

Grégoire Loupit[1] | Josep V. Fonayet[2,3] | Marcus D. B. B. Lorensen[4] | Céline Franc[2] | Gilles De Revel[2] | Christian Janfelt[4] | Sarah J. Cookson[1]

[1]EGFV, Univ. Bordeaux, Bordeaux Sciences Agro, Villenave d'Ornon, France

[2]Unité de recherche Oenologie, EA 4577, USC 1366 INRAE, ISVV, Université de Bordeaux, Villenave d'Ornon, France

[3]Bordeaux Metabolome Facility, MetaboHUB, PHENOME-EMPHASIS, Villenave d'Ornon, France

[4]Department of Pharmacy, Faculty of Health and Medical Sciences, University of Copenhagen, Copenhagen, Denmark

Correspondence

Sarah J. Cookson, EGFV, Univ. Bordeaux, Bordeaux Sciences Agro, INRAE, ISVV, Villenave d'Ornon F-33882, France.
Email: sarah.cookson@inrae.fr

Funding information

Institut Carnot Plant2Pro; Agence Nationale de la Recherche; European Regional Development Fund; European Cooperation in Science and Technology; Carlsbergfondet; Danish Council for Independent Research| Medical Sciences; Ministère de l'Education Nationale, de l'Enseignement Superieur et de la Recherche; European Union INTERREG POCTEFA

Abstract

Grafting is widely used in horticulture. Shortly after grafting, callus tissues appear at the graft interface and the vascular tissues of the scion and rootstock connect. The graft interface contains a complex mix of tissues, we hypothesised that each tissue has its own metabolic response to wounding/grafting and accumulates different metabolites at different rates. We made intact and wounded cuttings and grafts of grapevine, and then measured changes in bulk flavonoid, phenolic acid and stilbenoid concentration and used metabolite imaging to study tissue-specific responses. We show that some metabolites rapidly accumulate in specific tissues after grafting, for example, stilbene monomers accumulate in necrotic tissues surrounding mature xylem vessels. Whereas other metabolites, such as complex stilbenes, accumulate in the same tissues at later stages. We also observe that other metabolites accumulate in the newly formed callus tissue and identify genotype-specific responses. In addition, exogenous resveratrol application did not modify grafting success rate, potentially suggesting that the accumulation of resveratrol at the graft interface is not linked to graft union formation. The increasing concentration of complex stilbenes often occurs in response to plant stresses (via unknown mechanisms), and potentially increases antioxidant activity and antifungal capacities.

KEYWORDS

MALDI-MSI, perennial, rootstock, scion, *Vitis* spp, wounding

1 | INTRODUCTION

Grafting is a technique widely used in horticulture, particularly for perennials, and is increasingly used for annual plant production (Rouphael et al., 2010). This traditional technique makes it possible, by the combination of two tissues from two different plants, to form a single plant with the agronomical advantages of the scion and the rootstock genotypes (Mudge et al., 2009). The advantage of using grafting in agriculture is that we can independently select for desirable root and shoot traits.

Grafting uses the intrinsic capacities of plants to heal, which includes cell proliferation and dedifferentiation, allowing tissue reconnection, which is particularly at the vascular level (Hartmann et al., 2011; Melnyk, 2017). Grafting starts with a mechanical injury, which triggers

changes in plant metabolism and signalling, such as the production of reactive oxygen species and the activation of defence and wound healing mechanisms (Melnyk, 2017; Vega-Muñoz et al., 2020). In general, secondary metabolites accumulate at the graft interface during the months and years after grafting (Assunção, Pinheiro, et al., 2019; Canas et al., 2015; Musacchi et al., 2000; Usenik et al., 2006) and presumably these molecules have a role in plant defence mechanisms (Chong et al., 2009; Yang et al., 2018). In addition to biochemical changes, callus cells often proliferate at the graft union, symplastic connections are made via plasmodesmata, and the phloem and xylem connect between the scion and rootstock (Hartmann et al., 2011).

Although widely used, grafting is sometimes unsuccessful. These grafts are characterised by a low survival rate, weak graft unions and poor growth. Poor grafting success can have multifactorial origins such as the combination of certain scion/rootstock genotypes, poor grafting technique, the presence of pathogens in the grafted tissues or due to climatic conditions (Hartmann et al., 2011). Depending on the scion/rootstock combinations, the grafting success can therefore vary highly as well as from year to year. The genetic distance between the two grafted plants seems to be a determining factor in grafting success, however, tobacco (*Nicotiana benthamiana*) is high graft compatible with many different species, even with very distantly related ones (Notaguchi et al., 2020), although whether these grafts are truly functional, with connected vascular tissues, has not been determined. The origins of graft incompatibilities are difficult to elucidate, but research in this direction is essential because the use of new rootstocks could be a key factor of adaptation climate change for many agroecosystems (Ollat et al., 2015).

Many studies have attempted to identify metabolite markers of a successful graft union formation or graft incompatibility (Assunção, Pinheiro, et al., 2019; Canas et al., 2015; DeCooman et al., 1996; Errea, 1998; Hudina et al., 2014; Loupit et al., 2022), but with limited success (Loupit & Cookson, 2020). Epicatechin has been found in high concentrations at the graft interface of poorly compatible scion/rootstock combinations of grapevine approximately 3 months after grafting (Assunção, Pinheiro, et al., 2019) and pear/quince approximately 2 years after grafting (DeCooman et al., 1996). Loupit et al. (2022) investigated quantitative relationships between metabolite concentration around the graft interface and the grafting success rate, and found both positive and negative correlations between the concentration of different stilbenes and grafting success (Loupit et al., 2022). To our knowledge, no study has examined the changes in polyphenol concentration occurring around graft interface in the hours and days after grafting in any plant species, which is one of the objectives of the current study. In addition, the spatial distribution of polyphenols in the different woody tissues has been little studied, although a small number of papers have been published in recent years. For example, laser micro-dissection, dissection and metabolite imaging has been used to characterise the metabolite profiles of different tissues in tree species (Abreu et al., 2020; Hu et al., 2022; Yang et al., 2020), but few have examined metabolites in the bark and pith/heartwood. Furthermore, we know little of the tissue-specific metabolite changes triggered by wounding or grafting woody tissues in any plant species.

We have previously shown that certain metabolites, particularly stilbenes, accumulate at the graft interface of grapevine at least 1 month after grafting (Loupit et al., 2022; Prodhomme et al., 2019), but the spatiotemporal dynamics underlying these metabolite changes are not known. In this study, we combine a time course experiment on bulk tissue (using high performance liquid chromatography coupled with a triple quadrupole mass spectrometer [HPLC-QqQ]) and metabolite imaging (using matrix-assisted laser desorption/ionisation-mass spectroscopy imaging [MALDI-MSI]) to study the tissue-specific changes in metabolites occurring during graft union formation.

To characterise the temporal changes in polyphenols during grafting, we quantified several polyphenols above, below (representing the scion and the rootstock in grafted combinations) and at the graft interface at 0, 4 h, 1, 3, 6 and 15 days after grafting (DAG) in two hetero-grafts (*Vitis vinifera* cv. Pinot Noir [PN] on *Vitis riparia Michaux* cv. Riparia Gloire de Montpellier [RGM] and PN on *Vitis berlandieri x Vitis rupestris* cv. 140 Ruggeri [140Ru]). These time points were selected to characterise the early grafting responses, particularly the rapid accumulation of polyphenols. These two rootstocks were chosen for their differences in graft development: the rootstock 140Ru often produces grafts with a weak graft junction and large callus, whereas the rootstock RGM is highly graft compatible (Pl@ntGrape Database, 2009). In addition, to understand the genotype-specific metabolite responses to grafting, we studied the three homo-grafted controls of these genotypes (PN/PN, RGM/RGM and 140Ru/140Ru), as well as wounded and intact PN cuttings. We measured 41 polyphenols of interest (20 stilbenes, 14 flavanols, caftaric acid, coutaric acid, quercetin-3-glucoside, quercetin-3-glucuronide, naringenin, naringenin glucoside and taxifolin) in these samples. These compounds were selected based on the literature on the metabolites accumulated at the graft interface and their used as potential markers of compatibility (Assunção, Pinheiro, et al., 2019; Assunção et al., 2016; Canas et al., 2015; Loupit et al., 2022; Prodhomme et al., 2019).

The graft interface is complex, mixing two different genotypes, composed of different tissues (xylem, phloem, bark and pith) which are both intact and damaged, as well as the newly formed callus. Because of this, we hypothesised that each tissue have its own metabolic response to grafting and accumulate different metabolites. Therefore, to understand in which tissues the metabolites identified the time course experiment accumulate, we used MALDI-MSI to visualise metabolite spatial distribution at the graft interface at 16 and 30 DAG. MALDI-MSI is a useful tool to characterise the spatial distribution of metabolites (Bjarnholt et al., 2014). A number of studies have been done using MALDI-MSI on woody tissues particularly in conifers for example to study terpenoid metabolites (Abbott et al., 2010) and to compare the accumulation of coniferin in the xylem of normal and compression wood of cypress and cedar (Yoshinaga et al., 2016). Whereas fewer studies have been done in grapevine; for example, metabolite imaging has been used to determine the localisation of stilbenes after UV irradiation (Hu et al., 2022) or infection with *Plasmopara viticola* in leaves (Becker et al., 2014; Maia et al., 2022).

We have previously shown that resveratrol accumulates at the graft interface (Loupit et al., 2022; Prodhomme et al., 2019) and that

its concentration at the graft interface is positively correlated with grafting success (Loupit et al., 2022). To determine whether resveratrol has a role in grafting success, we exogenously applied resveratrol to the graft interface immediately after grafting and quantified grafting success after 1 year in the nursery.

2 | MATERIALS AND METHODS

2.1 | Plant material

Overwintering grapevine canes (lignified shoots of the year) were used to make the grafts and cuttings (Table 1); PN, 140 Ru and RGM were supplied by the Chambre de l'Agriculture de l'Aude (Carcassonne, France) except for MALDI-MSI analysis where RGM stems were supplied by Mercier (Vix, France). The HPLC-QqQ analysis was done in 2020 and the MALDI-MSI was done in 2022.

2.2 | Grafting procedure

Grapevine canes were stored in a fridge in 1 m long sections until shortly before grafting. For the time course experiment, 250 grafts were made for the five scion/rootstock combinations and 100 cuttings were made for each treatment. For the MALDI-MSI experiment, 100 grafts were made for each scion/rootstock combinations and 60 cuttings were made of RGM. One bud cuttings and 30 cm long de-budded cuttings were made for scions and rootstocks respectively. Just before grafting, all scions and rootstocks were rehydrated in tap water at room temperature for 4 h. Then all grafts were made using an Omega blade on a table top grafting machine (Omega Star, Chauvin, France). Immediately after grafting, the grafts were dipped in melted wax (Staehler Rebwachs pro with 0.0035% of dichlorobenzoic acid, Chauvin) and put in plastic boxes for 5 days at room temperature and then placed in callusing room (28°C and high humidity) with 2 cm of water in crates for 20–30 days depending on scion/rootstock combination.

For the time course experiment, at each date (0 and 4 h after grafting, and 1, 3, 6 and 15 DAG), five pools of five grafts and three pools of four cuttings were harvested randomly with pruning shears. Tissues were sampled at the graft interface, and 1 cm above and below the graft interface (without nodes) for the grafts, and 1 cm above, 1 cm below and at wounded interface for cuttings (in the case of PN intact cuttings, three different parts were sampled to correspond to the position of above, below and at the graft interface) corresponding to approximately 10 g of fresh tissue per biological replicate (Figure 1). All samples were immediately snap frozen in liquid nitrogen and kept at −80°C until analysis. Grafts remaining after harvesting for metabolite analysis were dipped in melted wax for a second time and planted in 5 L pots (filled with 50% sand and 50% potting compost (TERREAU MULTIPLICATION X31 from Dumona) with fertigation (N = 34.3; P = 17.7; K = 140.4; Ca = 74.9; Mg = 16.8; S = 41.4; Cl = 90.1 mg L^{-1}) and grown outside (near Bordeaux, France, 44°47′ N, 0°34′ W, elevation 22 m). On the 2 January 2021, the mechanical resistance of the graft union was tested to calculate grafting success rates for the five scion/rootstock combinations. Grafts were deemed successful if they did not break during the mechanical resistance test (Table 1).

For the MALDI-MSI experiment, two RGM cuttings and two grafts of each hetero-graft and homo-graft were studied at 0, 16 and 30 DAG. All samples were immediately snap frozen in liquid nitrogen and kept at −80°C until analysis.

TABLE 1 Scion/rootstock combinations used with grafting success rate in 2020 and Vitis International Variety Catalogue numbers in brackets.

Abbreviation	Scion genotype	Rootstock genotype	% of grafting success in 2020
Hetero-grafts			
PN/RGM	*Vitis vinifera* cv. Pinot Noir clone 115 (9279)	*Vitis riparia Michaux* cv. Riparia Gloire de Montpellier clone 1030 (4824)	60.3
PN/140Ru	*V. vinifera* cv. Pinot Noir clone 115 (9279)	*V. berlandieri* x *V. rupestris* cv. 140 Ruggeri clone 101 (10351) (clone 265 (10351) in 2022)	20.3
Homo-grafts			
PN/PN	*V. vinifera* cv. Pinot Noir clone 115 (9279)	*V. vinifera* cv. Pinot Noir clone 115 (9279)	6.25
RGM/RGM	*Vitis riparia Michaux* cv. Riparia Gloire de Montpellier clone 1030 (4824)	*Vitis riparia Michaux* cv. Riparia Gloire de Montpellier clone 1030 (4824)	28.1
140Ru/140Ru	*V. berlandieri* x *V. rupestris* cv. 140 Ruggeri clone 101 (10351) (clone 265 (10351) in 2022)	*V. berlandieri* x *V. rupestris* cv. 140 Ruggeri clone 101 (10351) (clone 265 (10351) in 2022)	32.8
Cuttings			
PN	*V. vinifera* cv. Pinot Noir clone 115 (9279)		
PN wounded	*V. vinifera* cv. Pinot Noir clone 115 (9279)		
RGM	*Vitis riparia Michaux* cv. Riparia Gloire de Montpellier clone 1030 (4824)		

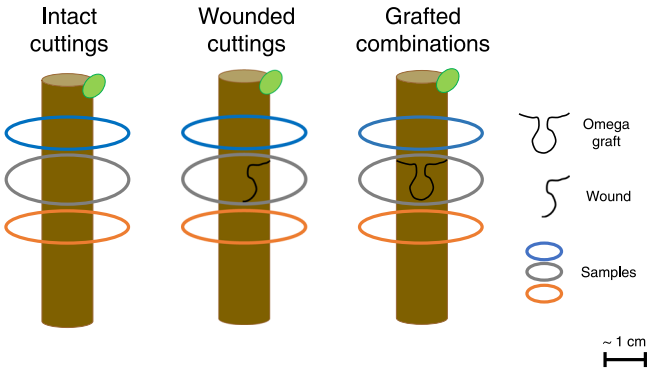

FIGURE 1 Experimental design. Sampling were taken from intact and wounded cuttings, grafted plants 0 and 4 h, and 1, 3, 6 and 15 days after grafting (DAG). At each time point, five pools of five grafts and three pools of four cuttings were harvested randomly. Colours represent samples of scions (blue), graft interfaces (grey) and rootstocks (orange).

An independent experiment was performed in 2021 to determine whether the application of resveratrol to the graft interface immediately after grafting could modify grafting success in a poorly compatible scion/rootstock combination. For this, over-wintering canes of *V. vinifera* cv. Ugni blanc (UB) and *V. berlandieri* x *V. riparia* cv. Rességuier Sélection Birolleau 1 (RSB1) (purchased from Mercier, Vix, France) were used to make UB/RSB1 heterografts and UB/UB and RSB1/RSB1 homografts. The grafting procedure was the same as above except that immediately after the scion and rootstock were cut, the cut surfaces of the scion and rootstock were dipped into a solution containing either water or resveratrol (2.5 g L^{-1}) for 5 s and then the graft was assembled manually. Grafting success was calculated 1 year after grafting.

2.3 | Chemicals and standards

All standards used came from Extrasynthesis (France) except for some stilbene monomers (*trans*-astringin and *trans*-isorhapontin), stilbene dimers (*trans*-ε-viniferin, *trans*-ω-viniferin, *trans*-δ-viniferin, pallidol, parthenocissin A, vitisinol C and ampelopsin A), stilbene trimers (miyabenol C and α-viniferin), and stilbene tetramers (hopeaphenol, isohopeaphenol, r2-viniferin and r-viniferin) which had been previously purified at the Bordeaux University (Enology Unit, 'Molécules à Intéret Biologique' laboratory, Villenave d'Ornon, France). Briefly, these stilbenes are isolated from grapevine woody parts using a combination of techniques including extraction with organic solvents, fractionation by Centrifugal Partition Chromatography, purification by preparative and semipreparative chromatography, and identification by HRMS and 1H-NMR (Papastamoulis et al., 2015; Pawlus et al., 2013). 1,5-Diaminonaphthalene (DAN, MALDI matrix) and carboxymethylcellulose sodium salt (CMC, embedding material), where both purchased from Sigma-Aldrich.

2.4 | Analysis by UHPLC-QqQ

Before extraction, fresh frozen samples were ground to powder in a ball mill (MM400 RETSCH) at 30 Hz during 30 s cooled with liquid nitrogen. The extraction protocol was the same as used by Loupit et al. (2022) (250 mg of ground powder extracted with 4 mL of methanol of 15 min in an ultrasound bath) (Loupit et al., 2022). Then, polyphenol analysis was done by multiple reaction monitoring (MRM) as described by Loupit et al. (2020) except that some additional compounds were added (Supporting Information: Table S1) as a different column was used (Agilent ZORBAX RRHD SB-C18 [2.1 mm × 100 mm, 1.8 µm]) (Loupit et al., 2020). The two solvents used were A (water/0.1% formic acid) and B (acetonitrile/0.1% formic acid), with a elution gradient for solvent B: 1%–10% (0–4 min), 10%–20% (4–12 min), 20%–30% (12–13 min), 30%–30% (13–16 min), 30%–35% (16–18 min), 35%–50% (18–20 min), 50%–95% (20–21 min). The flow rate was 0.4 mL/min. External standards, for build standard curves, were used to quantify the different compounds (concentration ranged from 0.01 to 20 mg L^{-1} and to 100 mg L^{-1} for catechin, epicatechin, B1, hopeaphenol, r-viniferin and *trans*-ε-viniferin) except for procyanidin B3, B4, *cis*-piceid, *cis*-astringin and coutaric acid were quantified as procyanidin B1, B2, *trans*-piceid, *trans*-astringin and caftaric acid respectively. Furthermore, one flavanol dimer and two flavanol trimers were given the names dimer, trimer2 and trimer3 respectively, and quantified as procyanidin B2 (for the dimer) and procyanidin C1 (for the trimers). The quantification was performed using the MassHunter Quantitative software (Agilent Technlogies) using the peak area of the quantifier ion for calibration and quantification and the qualifier ions ratio for identity confirmation (Supporting Information: Table S1). All concentration found are given as g kg^{-1} FW (Supporting Information: Data S1).

2.5 | Analysis by MALDI-MSI

Graft interfaces, cuttings and wood samples were embedded in a 2% CMC solution in Milli-Q water and kept at −80°C. Cryosectioning was performed as described by Granborg et al. (2022) by using a Leica CM3050S cryo-microtome (Leica Microsystems) at −25°C to make 20 µm thick longitudinal sections (adapted from Kawamoto [2003]), harvested at the middle of the graft (Granborg et al., 2022; Kawamoto, 2003). Sections were attached to microscope slides using double-sided graphite tape (Electron Microscopy Sciences) and then stored at −80°C until analysis.

Before matrix application, sections were dried for 20 min in a vacuum desiccator at room temperature. Then, 300 µL of matrix solution (3.3 mg mL^{-1} of DAN in 90:10 methanol:H_2O [v/v]) was applied at 30 µL min^{-1} using a pneumatic sprayer (the distance between sprayer and sample was 10 cm with a gas pressure of 2.0 bar and the sample was rotated at 600 rpm).

MALDI-MSI analysis was performed on a Thermo QExactive Orbitrap mass spectrometer (Thermo Scientific GmbH) equipped with an AP-SMALDI10 ion source (TransMIT GmbH) operated at a mass

resolving power of 140 000 at *m/z* 200, with a lock-mass from matrix peak of DAN (*m/z* 311.1302). The analysis was performed in negative-ion mode with a pixel size of 35 µm and using a range analysis between 100 and 1000 *m/z*. Finally, RAW files were converted to imzML files with RAW2IMZML software (TransMIT GmbH) and images were made with MSiReader ver. 1.02 (Bokhart et al., 2018; Robichaud et al., 2013) with normalisation to the total ion current (TIC) and a mass tolerance of 5 ppm. Two biological replicates for each condition were studied.

2.6 | Statistics analysis

HeatMaps were made on software R (version 4.0.4) and RStudio (version 1.2.5019) using gplots package. Statistical tests (*T*-test) were done online on BioStatFlow v.2.9.5 © INRAE 2022 to identify metabolites that accumulates specifically at the graft interface. Stars, positioned on time course data and HeatMaps, indicates only a significant difference between scion and graft interface, and between graft interface and rootstock. Significance threshold set at p-value < 0.05, with False Discovery Rate adjustment. All p-value for each scion/rootstock combinations and cuttings, over the time, are given in Supporting Information: Data S2. The effect of exogenous application of resveratrol on grafting success and grafting success rate for grafted combinations studied were tested with a Chi-squared test using R (Figure 7 and Supporting Information: Data S2).

3 | RESULTS

3.1 | Stilbenes accumulate at the graft interface

To investigate the temporal changes in polyphenols occurring during graft union formation in grapevine, we measured 41 metabolites in two hetero- and three homo-grafted scion/rootstock combinations above, below and at the graft interface at 0, 4 h, and 1, 3, 6 and 15 days after grafting. To identify metabolite profiles specific to grafting, we also compared the polyphenol responses to grafting and wounding in the PN genotype at the same time points after wounding. In addition, we measured metabolites in PN cuttings at the same location and time points as the tissues harvested for above, below and at the graft interface as intact controls. The sum of the flavanols and stilbenes in the different tissues provides an overview of the metabolites changes occurring (Figure 2). Total flavanol and stilbene concentration did not change in the stems of intact PN cuttings over the 15 days period (Supporting Information: Data S2). However, in all grafting or wounding treatments, stilbenes accumulated at the graft interface/wound site, while the quantity of flavanols remained stable or slightly decreased over time (Figure 2 and Supporting Information: Data S1 and S2). Total stilbene concentration reached a maximum at 6 DAG at the graft interface/wound site in all treatments compared to scion and rootstock tissues. Stilbene accumulation at the graft interface was significant at 3 DAG, whereas it was significant only at 6 DAG for wounded cuttings. The relative increase at the graft interface in relation to the surrounding woody tissues was higher in 140Ru/140Ru (approximately two-fold) compared to the other two homo-grafts (approximately 1.3-fold) (Supporting Information: Data S1 and S2). In addition, total stilbene content below and above the graft interface remained stable during the 15 DAG in 140Ru/140Ru, but increased by at least 1.7- and 1.5-fold in PN/PN and RGM/RGM homo-grafts respectively (Supporting Information: Data S1 and S2). The maximum total stilbene accumulation at the graft interface was higher in PN/PN homo-grafts compared to wounded PN cuttings, while the amount found at 1 DAG was similar in both conditions. Furthermore, the concentration of total stilbenes in the hetero-grafts depended on both the genotype-specific differences in stilbene concentration and the accumulation of total stilbenes at the graft interface and showed similar patterns to the homo-grafts.

The accumulation of the different stilbene compounds at the graft interface of the two hetero-grafts was globally similar except for certain compounds such as isorhapontigenin, pallidol, α-viniferin or miyabenol C (Supporting Information: Data S1). These differences seemed to be mainly due to genotype-specific differences in metabolite responses to wounding/grafting. For example, isorhapontigenin and α-viniferin are more highly accumulated at the graft interface of PN/140Ru than PN/RGM, this is primarily due to the high accumulation of these compounds by the 140Ru genotype. Similarly, pallidol and miyabenol C are more highly accumulated at the graft interface of PN/RGM than PN/140Ru, this is primarily due to the high accumulation of these compounds by the RGM genotype (Supporting Information: Data S1 and S2).

3.2 | Stilbene monomers accumulate from 1 DAG whereas complex stilbenes accumulate from later time points

To gain further insights into the accumulation of stilbenes at the graft interface, the sum of the different monomers (7), dimers (7), trimers (2) and tetramers (4) (Supporting Information: Table S1) was calculated (Figure 3). Concerning the intact PN cuttings, the concentration of the different stilbenes did not show significant differences in the sites of ''above', 'below' and at the 'graft interface'. However, the concentrations of stilbene monomers and dimers increased from 1 DAG to 6 DAG, trimers from 6 DAG and tetramers increased at 15 DAG (Figure 3).

Stilbene monomers, dimers and trimers accumulated to much higher levels at the wound site and graft interface in all scion/rootstock combinations in comparison to the surrounding woody tissues. The accumulation of monomers was continuous and significant from 1 DAG in the 140Ru and RGM homo-grafts and in the two hetero-grafts, and from 3 DAG in wounded cuttings and PN homo-grafts. This accumulation pattern was largely due to the accumulation of resveratrol, the major stilbene monomer in these tissues (Supporting Information: Data S1). However, at 15 DAG, the

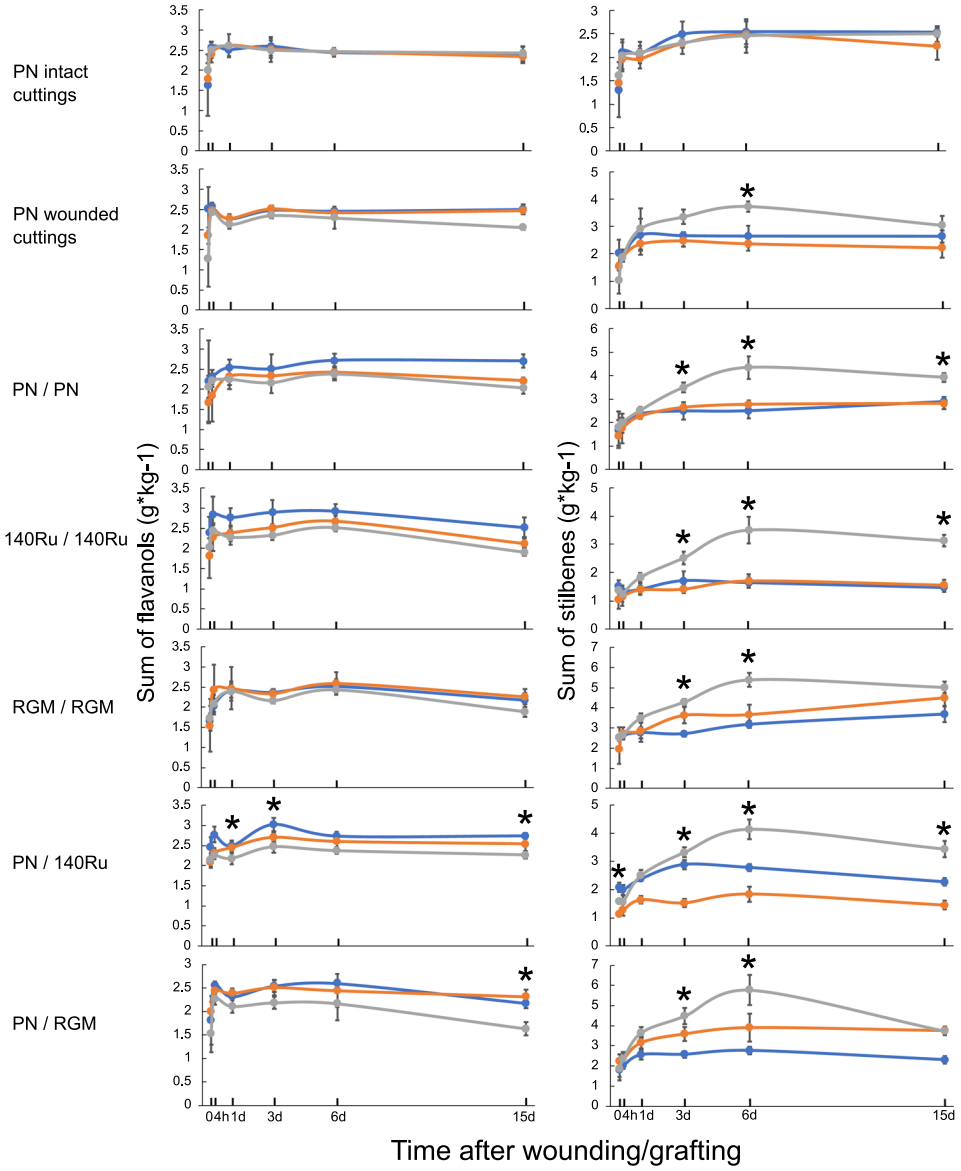

FIGURE 2 Effect of wounding and grafting on the sum of flavanols and stilbenes at 0 and 4 h, and 1, 3, 6 and 15 days after grafting/wounding grapevine stems. Intact and wounded cuttings of PN (*Vitis vinifera* cv. Pinot Noir) were studied, as well as various homo- and hetero-grafts of three grapevine genotypes (Pinot Noir [PN], Riparia Gloire de Montpellier [RGM] [*Vitis riparia* Michaux cv. Riparia Gloire de Montpellier] and 140 Ru [*Vitis berlandieri x Vitis rupestris* cv. 140 Ruggeri). Samples were taken above (blue), below (orange) and at the graft interface (grey). Error bars represent means ± the standard deviation ($n = 5$ for grafts and $n = 3$ for cuttings). Stars indicate a significant difference between scion and graft interface, and between graft interface and rootstock after a *T*-test analysis (with false discovery rate adjustment) with a significance threshold set at p-value < 0.05. [Color figure can be viewed at wileyonlinelibrary.com]

quantity of monomers decreased significantly in comparison to 6 DAG. In general, the accumulation of dimers, trimers and tetramers at the graft interface occurred later in the time course than the accumulation of monomers (Figure 3). Tetramers only accumulated at the graft interface towards the end of the time course and only in the PN/PN, PN/140 Ru and 140Ru/140Ru combinations (Figure 3).

Stilbene dimers were present in large quantities in all the tissues studied, due to the high content of *trans*-ε-viniferin (Supporting Information: Data S1). The level of accumulation of *trans*-ε-viniferin at the graft interface was strongly dependent on the scion and rootstock genotype. This is because stilbene dimer concentration was much lower in the canes used for grafting (at $T = 0$) of 140Ru than the other two genotypes (Figure 3). Furthermore, the relative increase in dimer concentration at the graft interface depended on the scion/rootstock genotypes; for example, in 140Ru homo-grafts, dimer concentration doubled from 0 to 15 DAG, whereas in RGM homo-grafts maximum dimer concentration was at 6 DAG and the relative increase was approximately 40% from 0 to 6 DAG (Supporting Information: Data S1).

The accumulation of trimers at the interface began at 3 DAG (except for combinations with the 140Ru genotype where it began from 1 DAG) and increased until 15 DAG (at least by two-fold) except

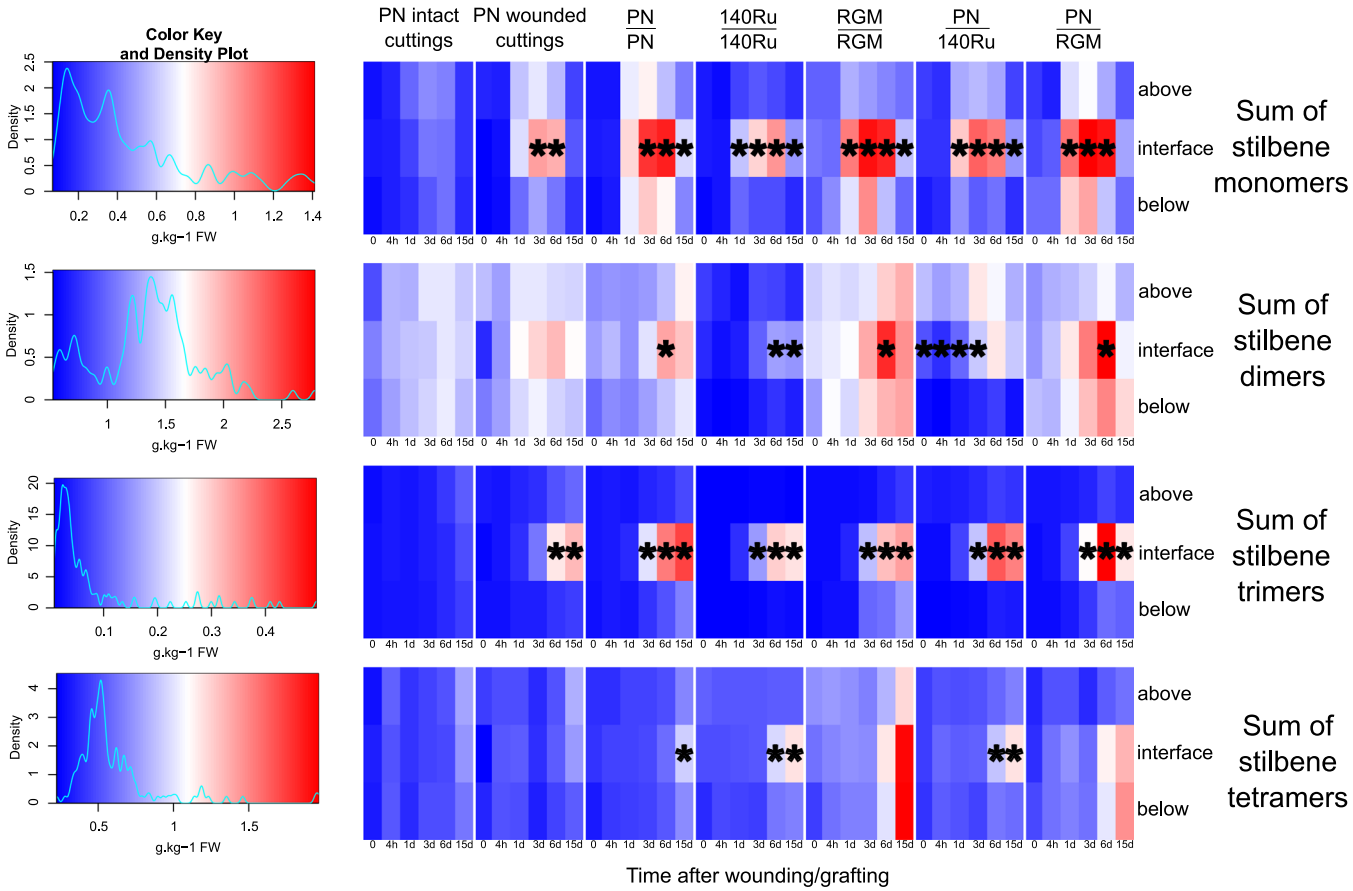

FIGURE 3 Unscaled heatmaps of the effect of wounding and grafting on sum of stilbene monomer, dimer, trimer and tetramer concentrations at 0 and 4 h, and 1, 3, 6 and 15 days after grafting/wounding grapevine stems. Cuttings and grafts as described in legend for Figure 1. Stars indicate a significant difference between scion and graft interface, and between graft interface and rootstock, for each time point, after a *T*-test analysis with a significance threshold set at p-value < 0.05. [Color figure can be viewed at wileyonlinelibrary.com]

for PN/RGM (Figure 3). Finally, only 140Ru/140Ru and PN/PN homo-grafts and PN/140Ru hetero-grafts showed an increase of stilbene tetramers at 6 or 15 DAG at the graft interface compared to above and below it. Although tetramers did not accumulate at the graft interface of RGM/RGM homo-grafts and PN/RGM, they accumulated below the graft interface (Figure 3), especially for hopeaphenol and isohopeaphenol (Supporting Information: Data S1).

3.3 | Naringenin, taxifolin and compounds with a gallate residue also accumulate at the graft interface

The quantification of phenolic acids, flavonols and flavanols during the first 15 DAG showed significant differences between the genotypes and/or graft combinations studied, but no specific accumulation at the graft interface or wound site occurred except for naringenin and its glucoside form, taxifolin, and flavanol compounds with a gallate residue (Figure 4, Supporting Information: Data S1). These compounds were at the same concentrations in the different parts of intact PN cuttings, showing that the accumulation was specific to wounding or grafting despite the very low quantities measured. In all grafts and wounded cuttings, a strong accumulation of naringenin at the wound site began from 1 DAG (e.g., in 140Ru/140Ru homo-grafts at 1 DAG its concentration was 3 times higher at the interface compared to the scion and rootstock). However, this strong and rapid accumulation decreased over time until it was no longer significant at 15 DAG in wounded PN cuttings, PN/PN and RGM/RGM homo-grafts, as well as in PN/RGM hetero-grafts (Figure 4 and Supporting Information: Data S2). The accumulation pattern was similar for taxifolin except for 140Ru/140Ru homo-grafts, which accumulate high concentrations of taxifolin that remain high for longer than the other scion/rootstock combinations. Flavanols with a gallate residue also accumulated at the graft interface and wounding site, but only from 3, 6 or 15 DAG (Figure 4), the differences observed were largely due to differences in the accumulation of epigallocatechin gallate (Supporting Information: Data S1).

3.4 | The spatial distribution of polyphenols in different tissues of wood stems of grapevine

The use of MALDI-MSI allowed us to observe the spatial distribution of different compounds at different times after grafting (at 0, 16 and

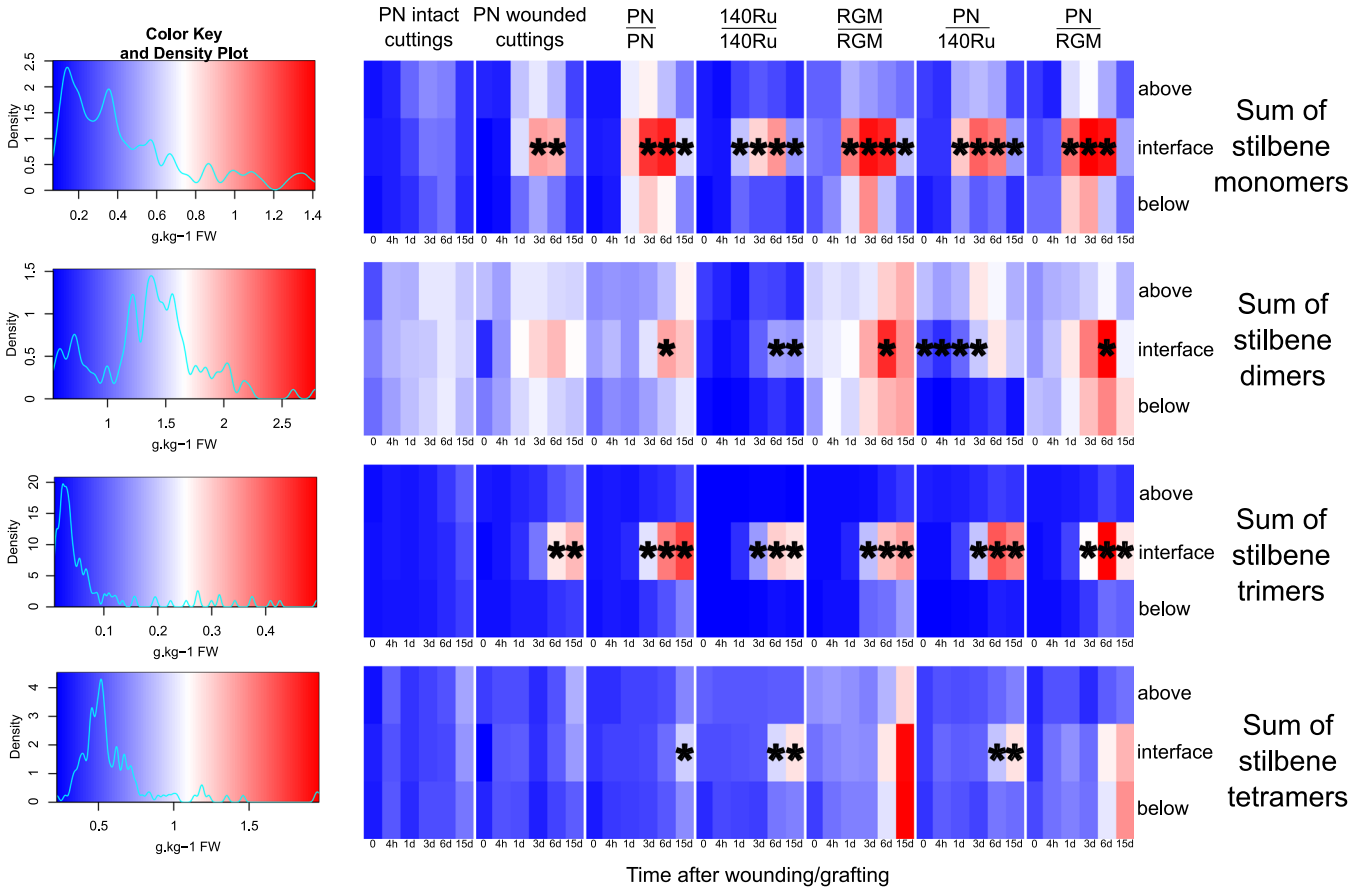

FIGURE 3 (Continued).

30 DAG). In PN, 140Ru and RGM wood (at 0 DAG), stilbenes (such as resveratrol, dimers, α-viniferin and tetramers) were found between the xylem part and the pith, as well as between the bark and phloem. In general, the distribution of these metabolites between the different tissues was similar between the different genotypes. However, in PN (Supporting Information: Tables S4 and S5), resveratrol, stilbene dimers, α-viniferin and tetramers are more highly concentrated in the pith, and tetramers seemed to be at lower concentration in the bark compared to 140Ru (Supporting Information: Tables S2 and S3) and RGM (Supporting Information: Tables S6 and S7). Concerning flavanol monomers (catechin, epicatechin) and flavanol dimers (B1, B2, B3, B4, etc...), we found a similar tissue-specific distribution to that of the stilbenes, except that flavanols were more highly concentrated in the pith and in their distribution was more homogeneous. However, for PN, flavanols were also present in high concentrations in the xylem and phloem tissues (Supporting Information: Tables S4 and S5). The distribution of taxifolin and naringenin was similar to that of the other compounds studied, with high concentrations in the pith and bark, and high concentrations of naringenin also in the xylem area of PN (Supporting Information: Tables S4 and S5). Despite these small differences in metabolites distribution patterns, overall the localisation of the different metabolites of interest was similar between genotypes.

3.5 | Stilbenes accumulate in wounded tissues while naringenin, taxifolin and epigallocatechin gallate accumulate in callus

Flavanol monomers and dimers did not accumulate at the graft interface in any of the grafts studied. These compounds were distributed in the same fashion as in the cuttings at 0 DAG. However, these compounds accumulate to low levels in the newly formed callus at 30 DAG (Supporting Information: Tables S2–S11).

Concerning resveratrol, we observed an accumulation at 16 DAG along the zone of the cut surfaces at the graft interface, which corresponds to the omega shape of the grafting machine (Figures 5a and 6a). This accumulation was clearly visible, particularly in the xylem parenchyma tissues in the PN and RGM genotypes, and in hetero-graft and homo-graft combinations. Conversely, in 140Ru genotype, the accumulation was throughout the xylem zone, but also in the pith (Figure 5a and Supporting Information: Tables S2 and S3). The localised accumulation of resveratrol in the cut tissue of the graft interface was generally less visible at 30 DAG in most grafts, except for RGM/RGM homo-grafts (Supporting Information: Tables S6 and S7). Stilbene dimers had similar distribution to resveratrol in hetero-graft combinations

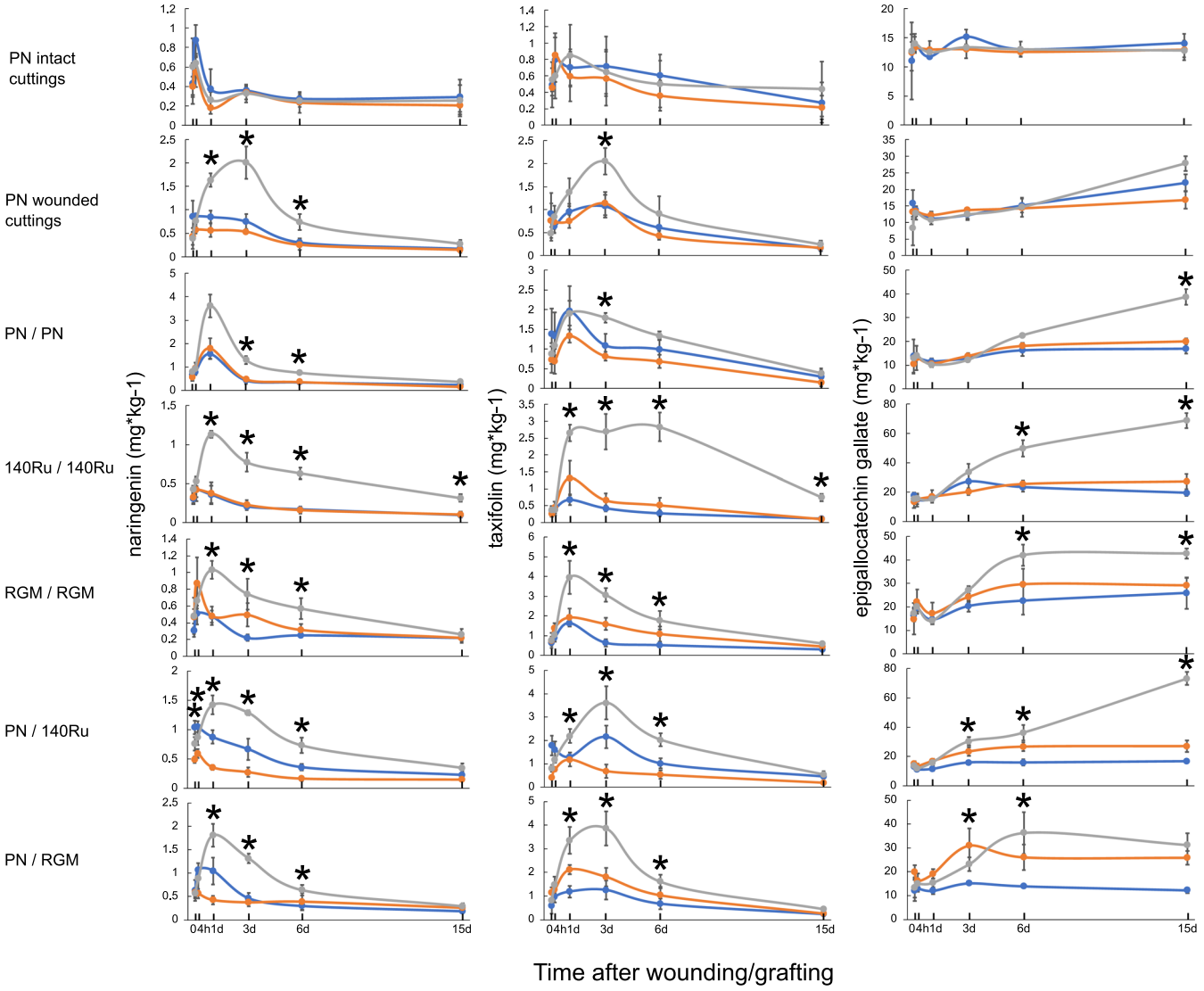

FIGURE 4 Effect of wounding and grafting on naringenin, taxifolin and epigallocatechin gallate concentration at 0 and 4 h, and 1, 3, 6 and 15 days after grafting/wounding grapevine stems. Cuttings and grafts as described in legend for Figure 1. Error bars represent means ± the standard deviation ($n = 5$ for graft combination and $n = 3$ for cuttings). Samples were taken above (blue), below (orange) and at the graft interface (grey). Stars indicate a significant difference between above and at the graft interface, and between below and at the graft interface (*T*-test analysis, with false discovery rate adjustment, p-value < 0.05). [Color figure can be viewed at wileyonlinelibrary.com]

(Supporting Information: Tables S8–S11), but seemed to accumulate less specifically at the interface in homo-grafted controls (Supporting Information: Tables S2–S7) whatever the time after grafting studied.

To determine the role of resveratrol during graft union formation, the cut surfaces of scions and rootstocks were dipped into a resveratrol solution (Figure 7). The resveratrol treatment did not alter grafting success in any of scion/rootstock combination tested.

Concerning the concentration of stilbene trimers such as α-viniferin, in grafted tissues α-viniferin was most concentrated in the xylem part, along the damaged tissues as well as around the xylem vessels, but it was absent from the pith (Figures 5 and 6). In 140Ru genotype, α-viniferin was highly concentrated between the xylem part and the pith, whereas in PN and RGM genotypes, this observation was not so apparent. Concerning the stilbene tetramers, their distribution is similar to those of other stilbenes: an accumulation was visualised along the interface at 16 DAG in the hetero-grafts, but it seemed to disappear at 30 DAG. Moreover, unlike dimers or resveratrol and the wood at 0 DAG, the presence of stilbene tetramers was not visible between the bark and the phloem part (Supporting Information: Tables S8–S11). In some cases, especially in PN genotype, resveratrol, dimers and trimers also accumulated at the outer edge of the callus.

The visualisation by MALDI-MSI showed that epigallocatechin gallate, naringenin, and taxifolin accumulate at the graft interface at 16 DAG (Figure 4, Supporting Information: Tables S2–S11). In all grafts,

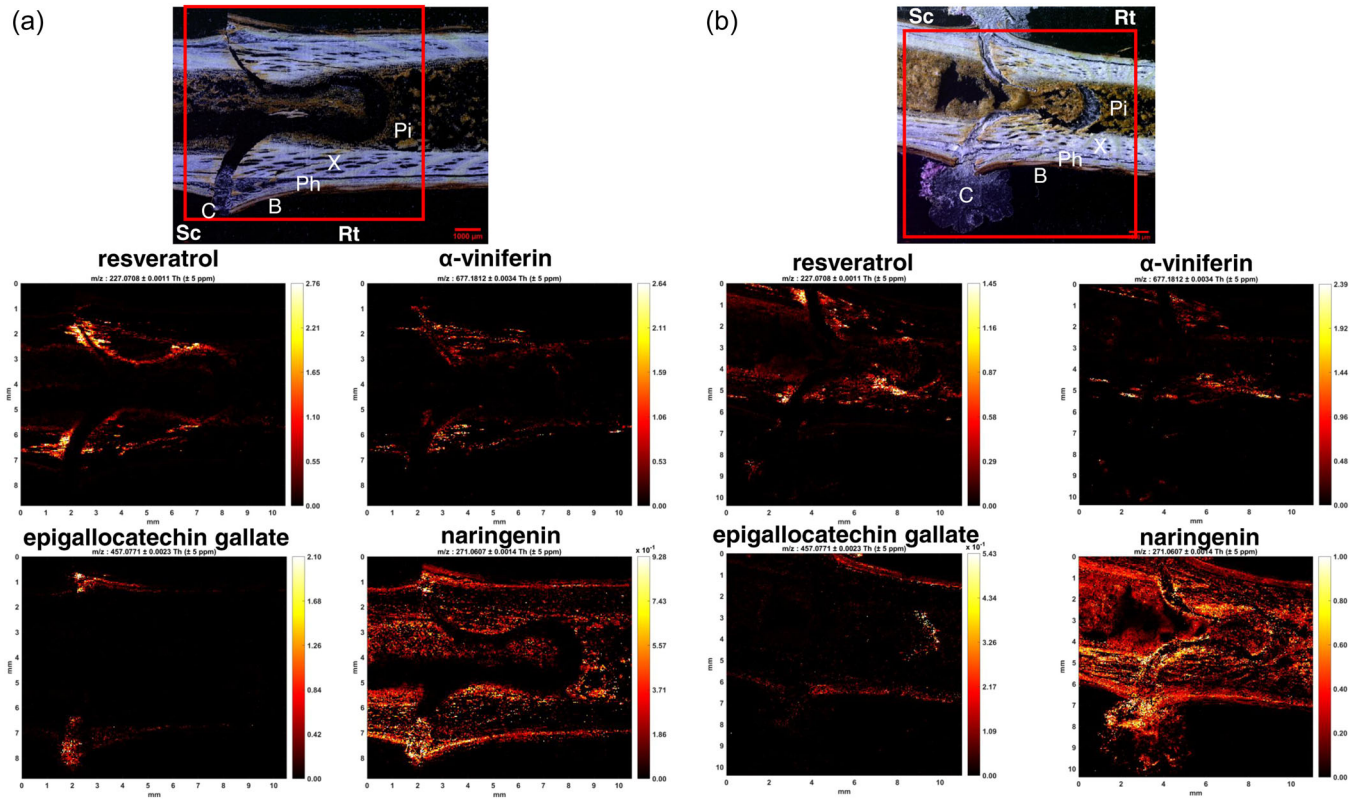

FIGURE 5 Representative photographs of *Vitis vinifera* cv. Pinot Noir/*Vitis berlandieri x Vitis rupestris* cv. 140 Ruggeri hetero-grafts sections at (a) 16 and (b) 30 days after grafting (DAG) and their mass spectroscopy (MS) images generated for *m/z* 227.0708, *m/z* 677.1812, *m/z* 457.0771 and *m/z* 271.0607 corresponding to resveratrol, α-viniferin, epigallocatechin gallate and naringenin respectively. The red boxes correspond to the area analysed. Sc, scion; Rt, rootstock; C, callus; B, bark; Ph, phloem; X, xylem; Pi, pith. [Color figure can be viewed at wileyonlinelibrary.com]

epigallocatechin gallate was found specifically accumulated in callus at 16 DAG, however at 30 DAG it has a more diffuse distribution across the tissues (Supporting Information: Tables S2–S11). Naringenin or taxifolin were easily visible with MALDI-MSI and were widely distributed in the tissues, these compounds accumulated to high levels in the callus tissues (Supporting Information: Tables S2–S11), but also along the cut tissues of the graft interface, in particular at 30 DAG in the pith in PN/140Ru hetero-grafts and RGM homo-grafts (Figure 5b, Supporting Information: Tables S6 and S7).

4 | DISCUSSION

The objective of this study was to characterise the spatiotemporal changes in polyphenols occurring at the graft interface during graft union formation in grapevine, a woody perennial crop species. This is important firstly because much research effort has been devoted to identifying metabolite markers of poor graft union formation and graft incompatibility with limited success (Loupit & Cookson, 2020), and secondly, because many genes related to polyphenol synthesis are induced during graft union formation (Assunção, Santos, et al., 2019; Cookson et al., 2013) and the function of these metabolites is unknown.

4.1 | trans-ε-viniferin is the major stilbene in grapevine canes and is heterogeneously distributed in grapevine stem tissues

The polyphenol found in highest concentration in the tissues studied was *trans*-ε-viniferin, a dehydrodimer, which is formed by the oxidative dimerisation of resveratrol (Supporting Information: Data S1). *trans*-ε-viniferin was also found to be the major stilbene in other studies on the graft interface of grapevine (Loupit et al., 2022; Prodhomme et al., 2019), as well as in grapevine canes (Billet et al., 2018; Loupit et al., 2020). *trans*-ε-viniferin, like other stilbenes, is known to be a phytoalexin, and therefore to have strong antioxidant and antifungal capacities (Chong et al., 2009). The high levels of stilbenes present in the woody tissues of grapevine could function as a constitutive protection mechanism for these perennial tissues against both abiotic stresses and pathogens.

4.2 | Grapevine genotypes have different wood metabolite profile

We have previously shown that there is a large degree of variation in cane metabolite profile across different *Vitis* spp. (Loupit et al., 2020). However, the three genotypes studied had broadly similar metabolite

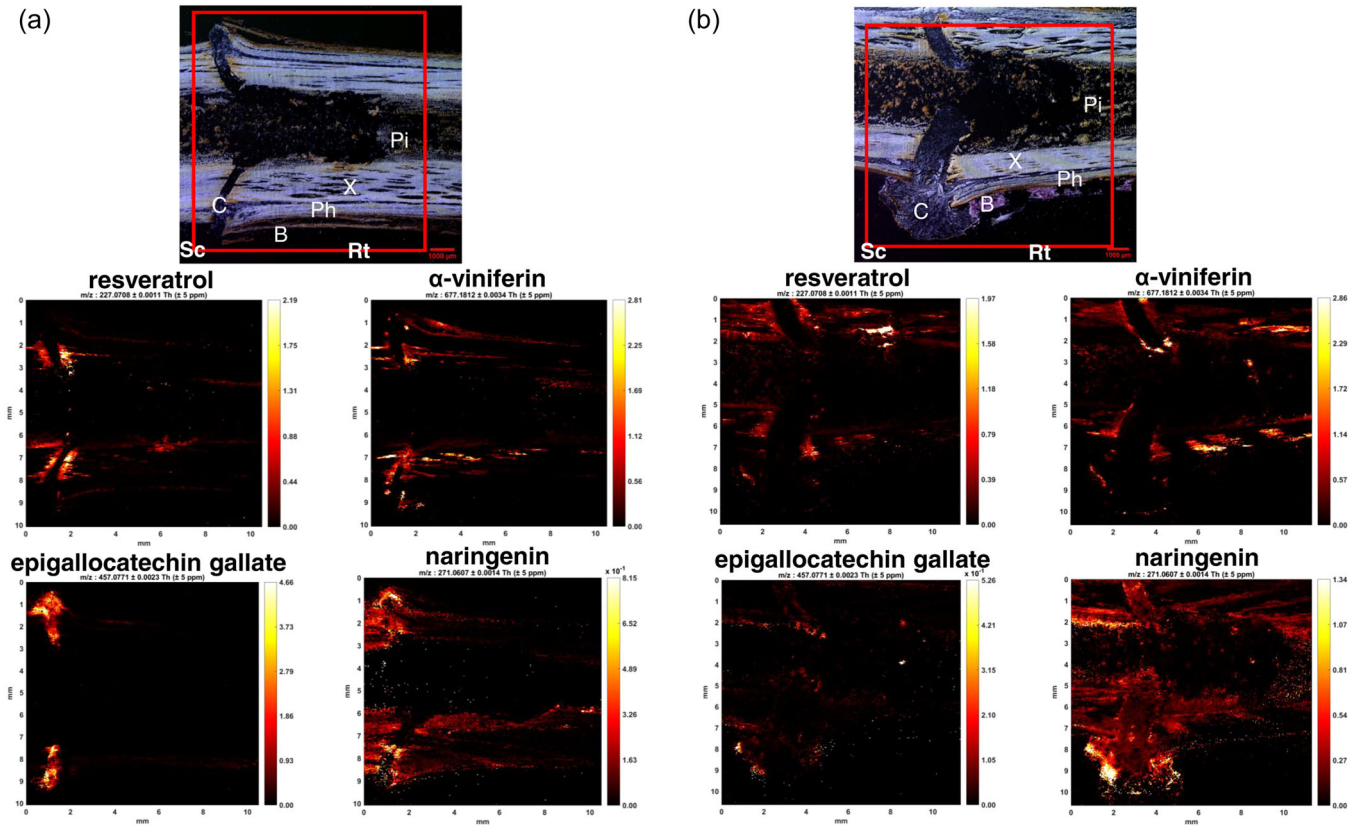

FIGURE 6 Representative photographs of *Vitis vinifera* cv. Pinot Noir/*Vitis riparia* Michaux cv. Riparia Gloire de Montpellier hetero-grafts sections at (a) 16 and (b) 30 days after grafting (DAG) and their mass spectroscopy (MS) images generated for *m/z* 227.0708, *m/z* 677.1812, *m/z* 457.0771 and *m/z* 271.0607 corresponding to resveratrol, α-viniferin, epigallocatechin gallate and naringenin respectively. The red boxes correspond to the area analysed. Sc, scion; Rt, rootstock; C, callus; B, bark; Ph, phloem; X, xylem; Pi, pith. [Color figure can be viewed at wileyonlinelibrary.com]

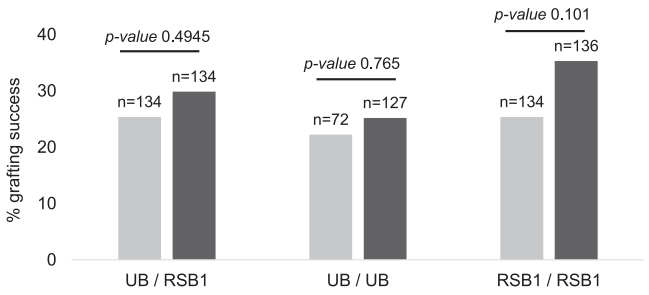

FIGURE 7 Effect of resveratrol (in black) treatment (2.5 g L^{-1}) and water (in grey) as control on grafting success rate of *Vitis vinifera* cv. Ugni Blanc (UB)/*Vitis berlandieri x Vitis riparia* cv. RSB1, UB/UB and RSB1/RSB1. No differences were found by using Chi-squared tests. Number of grafts and *p*-value are given in labels.

profiles (Supporting Information: Data S1) except that 140Ru has lower stilbene concentrations than the other two genotypes studied, in grafted and un-grafted conditions, which in particular was due to its relatively low concentration of stilbene dimers (Figures 2 and 3). This could be because we studied grafting in commercially grafted scion and rootstock genotypes, which corresponds to a relatively limited range of genetic (and metabolomic, Loupit et al., 2020) diversity. MALDI-MSI showed that stilbenes were most concentrated in the bark, pith and between the pith and xylem zones (Supporting Information: Tables S2 and S13). In RGM and PN wood, stilbene dimers and α-viniferin were distributed throughout the pith, whereas in 140Ru these metabolites were largely restricted to the pith/xylem boundary (Supporting Information: Tables S4–S7).

In the wood of poplar, phenylalanine, one of the central amino acids involved in the phenylpropanoids biosynthesis, is localised in the cambium and new xylem formed, potentially explaining the high concentrations of stilbenes in the xylem part (Abreu et al., 2020). However, catechin, which also comes from phenylalanine pathway, was mainly localised in the phloem and cambium tissue of grapevine and largely absent from the xylem area, in agreement with results on poplar in which catechin was also absent from the xylem area (Abreu et al., 2020).

4.3 | Some metabolites changes over time, which we hypothesise is related to spring reactivation of growth

The concentrations of the different compounds in the intact control cuttings were not significantly different between the parts above,

below and at the interface, which indicates that the sampling zone under the bud has no influence on metabolite quantification. However, a slight increase in stilbenes and some other compounds was observed over time in the three areas sampled (Figures 2–4 and Supporting Information: Data S1 and S2). An increase in stilbene concentration over time was also observed in the wood above and below the graft interface in the grafts of PN and RGM, whereas these metabolites did not change in the wood above and below for 140Ru homo-grafts and hetero-grafts (Figure 2 and Supporting Information: Data S2). During the 15 DAG, there is a reactivation of the metabolism due to the breaking of dormancy and bud burst, which involves many changes in primary and secondary metabolism, and metabolism-related gene expression (Noronha et al., 2021). For example, the transcript abundance of 12 stilbene synthases increases after the transfer of grapevine cuttings to warm dormancy release conditions (Noronha et al., 2021). The genotype-specific changes in cane metabolite concentration could be related to their responses to spring reactivation of growth; *V. vinifera* (PN) and *V. riparia* (RGM) are considered as low chill requiring, rapid bud bursting grapevine species, whereas *V. rupestris* (one of the parents of 140Ru) generally have higher chill requirements and slower bud break (Londo & Johnson, 2014).

4.4 | Grafting and wounding induce a rapid and transient accumulation of naringenin and taxifolin, which are mainly present in callus

The concentration of naringenin and taxifolin rapidly and transiently increased at the graft interface/wounding site (Figure 4), these compounds are intermediate metabolites and precursors in flavonoid biosynthesis. Naringenin and taxifolin are localised in the callus tissues 16 DAG (Figures 5 and 6 and Supporting Information: Tables S2–S11), but as callus tissues are absent in the first few days after grafting, they presumably accumulate in the tissues damaged during wounding produce by grafting process. In addition to being intermediates in the synthesis of flavonoids, naringenin has also been identified as an allelochemical in annual species, for example in soya bean, naringenin is an activator of reactive oxygen species (ROS), salicylic acid and pathogen resistance, and is a signal molecule involved in root symbiosis with microorganisms (Dardanelli et al., 2010). The application of naringenin to roots inhibits vegetative growth and decreases lignin content in rice, maize and early barnyard grass (Deng et al., 2004). Although naringenin treatment to a culture solution of bean seeds improved tolerance to oxidative stress by inducing some enzymes with antioxidant activity, such as superoxide dismutase and catalase decreasing ROS content and reducing lipid peroxidation (Ozfidan-Konakci et al., 2020; Yildiztugay et al., 2020). This could suggest that naringenin could play a role during the early stages of graft union formation by increasing oxidative stress tolerance after wounding or grafting. In Norway spruce, taxifolin is synthesised by a flavanone-3-hydroxylase enzyme and induced resistance to bark beetles (Hammerbacher et al., 2019). Furthermore, taxifolin accumulates in developing xylem and phloem around cambial zone (Hammerbacher et al., 2019), consistent with our results showing the presence of taxifolin in callus, where new vascular connexions are actively being formed. Recently, An et al. (2023) proposed a regulatory network regulating flavonoid accumulation under post-harvest physiological deterioration (PPD) in tuberous roots of *Manihot esculenta* Crantz, and observed that naringenin concentrations increased during PPD (An et al., 2023).

4.5 | Flavanols do not seem to play a role during the first 2 weeks after wounding/grafting

A significant decrease in flavanol concentration was observed after wounding cuttings and at the graft interface of the two hetero-grafts compared to surrounding tissues, while the sum of total flavanols was stable over time in the intact control (Figure 2). Lower concentrations of epicatechin at the graft interface in comparison to the surrounding woody tissues 1 month after grafting has been reported previously (Prodhomme et al., 2019). This could be because these metabolites are oxidised and degraded in response to wounding or grafting. It is therefore possible that a decrease in epicatechin content at the graft interface is due to its role as ROS-scavenging and as an antioxidant compound but is not synthesised fast enough to maintain tissue epicatechin concentrations. Some studies in grapevine (Assunção, Pinheiro, et al., 2019; Canas et al., 2015) and in pear or apricot (Hudina et al., 2014; Musacchi et al., 2000; Usenik et al., 2006) have indicated that catechin and epicatechin could be used as markers of graft incompatibility. For example, the study of Canas et al. (2015) suggested that catechin could be an incompatibility marker for incompatible Syrah clones 1 month after grafting (Canas et al., 2015), however, we did not observe a spatial distribution of catechin at the graft interface consistent with this hypothesis. Furthermore, we did not identify significant differences in flavanol concentration or distribution between the two hetero-graft combinations studied, which are known to have different grafting success rates (Pl@ntGrape Database, 2009, Table 1). The lack of agreement between these results could be because different types of graft failure (i.e. incompatibly related to the scion Syrah or poor grafting success with the rootstock 140Ru) could lead to the production of different metabolites at the graft interface.

4.6 | Gallate-compounds accumulate over the time and in the callus

Although most flavanols did not accumulate at the graft interface, flavanols with a gallate residue, such as epigallocatechin gallate, did accumulate at the graft interface and were shown to accumulate particular in the callus tissue (Figures 4–6 and Supporting Information: Table S2–S11). Flavanols are also known for their strong antioxidant capacity and it has already been shown that

epigallocatechin, epigallocatechin gallate or even epicatechin gallate have higher antioxidant capacities than flavanol monomers or gallic acid alone (Rice-Evans, 1995). No accumulation of flavanol gallates was reported in leaves during the first hours and days after wounding (Chitarrini et al., 2017), while we were able to detect a rapid accumulation, even when no callus was formed. This could suggest that wounding responses in leaves and woody stems induces the production of different defence metabolites.

4.7 | Stilbene accumulation is higher in grafted than wounded stems

The sum of total stilbenes increased in response to both wounding and grafting in all genotypes studied (Figure 2), this agrees with our previous studies on graft union formation in a wide range of scion and rootstock genotypes (Loupit et al., 2022; Prodhomme et al., 2019). Total stilbenes (as well as monomers and the different stilbene oligomers) accumulated to higher levels in the PN/PN homo-grafts than in the wounded PN cuttings relative to the intact cuttings (Figure 2 and Supporting Information: Data S2). This could suggest that either the larger the wound the higher the stilbene accumulation or that a full cut across the stem triggers a higher stilbene accumulation than a partial cut. In perennial species, secondary metabolites are known to be accumulated in xylem parenchyma in response to abiotic or biotic stresses (Morris et al., 2020). This metabolic response is one part of the Compartmentalisation of Decay in Trees (CODIT) Model, which aims to limit pathogen infections in perennial plant structures. The CODIT model considers that the xylem parenchyma is an important barrier to pathogens and produces phytoalexins in response to stress, limiting or compartmenting ROS and pathogen infections (Słupianek et al., 2021). The accumulation of defence-related compounds after wounding or grafting could have a role in protecting the healthy tissues from pathogen infection. The wood metabolite profile of grapevine, in particular the ability to produce resveratrol and viniferins after wounding, has been linked to resistance to Botryosphaeriaceae-related dieback (Khattab et al., 2021), suggesting that these metabolite differences have consequences for plant function.

Although resveratrol accumulates to high levels after grafting, we found that exogenous resveratrol application to the graft interface did not alter grafting success in the scion/rootstock genotypes tested (Figure 7). To our knowledge, this is the first time that the effect of exogenous application of a stilbene compound on wounding or grafting responses has been tested. However, exogenous application of a polyphenol-rich extract on has mixed effects on grafting success and callus formation (Volf et al., 2006). In other contexts, exogenous resveratrol has been shown to enhance growth, abiotic stress adaptation, and decrease oxidative damage by inducing several antioxidant enzymes (Santos Wagner et al., 2022), but stilbenes can also inhibit plant development (Seigler, 2006), making these compounds complex regulatory chemical signals (Chong et al., 2009).

4.8 | Stilbene monomers accumulate rapidly after wounding/grafting while complex stilbenes generally accumulate a later time points

In general, stilbene monomers and dimers increased from 1 DAG, trimers from 6 DAG and tetramers increased at 15 DAG (Figure 3). At the end of the time course, stilbene monomer concentrations decreased at the graft interface (from 3 or 6 to 15 DAG) (Figure 3 and Supporting Information: Data S2); this could suggest that these monomers were used to form oligomers or are degraded over time. The sequential appearance of stilbene monomers and then oligomers was also found in a study on metabolite changes in grapevine leaves after wounding (Chitarrini et al., 2017). The biosynthetic pathway of complex compounds is currently unknown, which does not allow us to know whether these compounds are actively formed by the plant, or passively accumulated. One of the hypotheses would be that the monomers oligomerize over time via their oxidation. The synthesis of resveratrol dimer has been carried out using in vitro oxidative coupling (El Khawand et al., 2020). In addition, oxidative oligomerization can occur via enzymatic reactions with horseradish peroxidase (Wilkens et al., 2010) or laccase-like stilbene oxidase from Botrytis cinerea (Breuil et al., 1998), although there is no direct evidence of these enzymes catalysing the oxidative oligomerization of stilbenes in plants.

4.9 | Metabolite markers of graft compatibility

Few differences were found in stilbene concentration between the two hetero-grafts with very different grafting success rates (60.3% for PN/RGM and 20.3% for PN/140Ru [Table 1 and Supporting Information: Data S2]), except that higher pallidol and miyabenol C concentrations were measured in PN/RGM compared to PN/140Ru (Supporting Information: Data S1 and S2). A similar trend was also observed in homo-grafts with higher grafting success rates (RGM/RGM and 140Ru/140Ru had grafting success rates of 28.1% and 32.8% respectively) in comparison with PN homo-grafts with lower grafting success rates (6.25%) (Table 1 and Supporting Information: Data S2). Conversely, α-viniferin was found in higher concentrations in grafts with low grafting success rates (Table 1 and Supporting Information: Data S1 and S2). In agreement with this observation, we have shown that this trimer is negatively correlated with grafting success in homo-graft combinations and it was identified as a potential graft incompatibility marker (Loupit et al., 2022). In addition, resveratrol concentration at the graft interface 1 month after grafting was also previously identified as a compound positively correlated with grafting success (Loupit et al., 2022). We also found that resveratrol increased to higher concentrations in the hetero-graft with this highest grafting success (PN/RGM) compared to the hetero-graft with lower grafting success (PN/140Ru) at 3–6 DAG (Supporting Information: Data S1). However, the concentration of resveratrol 15 DAG was not different between the different scion/rootstock combinations. Identifying robust and stable metabolite markers of

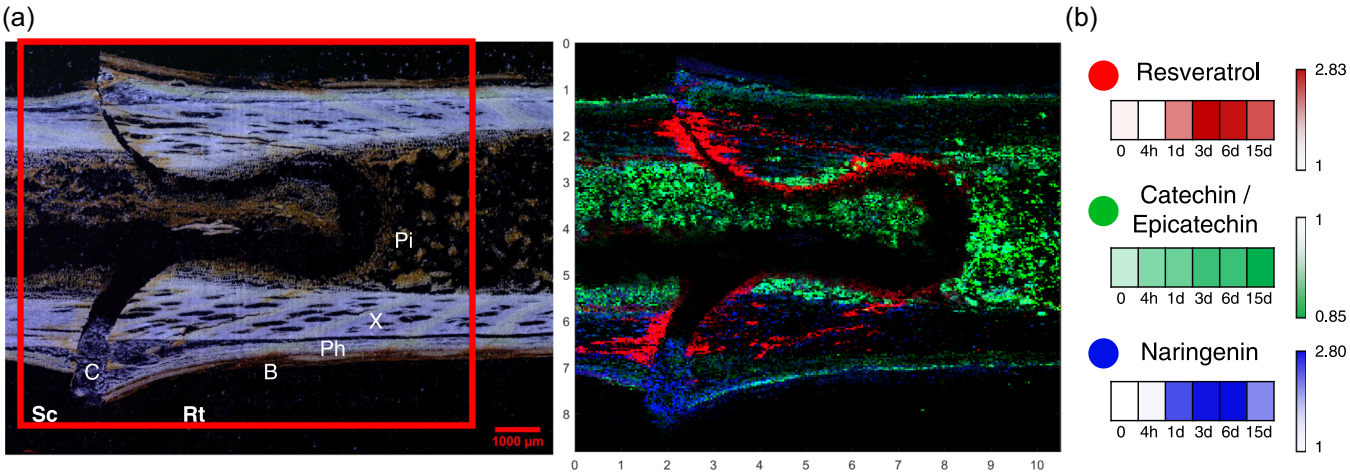

FIGURE 8 Summary of the (a) spatial and (b) temporal changes in resveratrol, catechin/epicatechin and naringenin at the graft interface during the first two weeks after grafting. (a) The section shown is of *Vitis vinifera* cv. Pinot Noir/*Vitis berlandieri x Vitis rupestris* cv. 140 Ruggeri., mass spectroscopy (MS) image generated for *m/z* 227.0708, *m/z* 289.0712 and *m/z* 271.0607 corresponding to resveratrol (red), catechin/epicatechin (green) and naringenin (blue) respectively. Data came from matrix-assisted laser desorption/ionization-mass spectroscopy imaging (MALDI-MSI) analysis. The red box corresponds to the area analysed. Sc, scion; Rt, rootstock; C, callus; B, bark; Ph, phloem; X, xylem; Pi, pith. (b) Heatmaps of ratios between the graft interface and the surrounding woody tissues (mean of above and below the graft interface)at 0 and 4 h, and 1, 3, 6 and 15 days after grafting. Data came from high-performance liquid chromatography coupled with a triple quadrupole mass spectrometer (HPLC-QqQ) analysis. [Color figure can be viewed at wileyonlinelibrary.com]

grafting success or compatibility is challenging (Loupit & Cookson, 2020), the spatiotemporal characterisation of metabolite changes occurring during graft union formation underlines the complexity of this challenge.

5 | CONCLUSION

The objective of this study was to resolve the temporal changes in polyphenol concentration underlying graft union formation and to characterise the spatial distribution of these metabolites. Few studies have looked at the kinetics of the accumulation of polyphenols in response to wounding/grafting in grapevine except for one study on metabolites changes in leaf discs during the first 120 h after wounding (Chitarrini et al., 2017). The comparison of metabolites accumulated after wounding in leaf and woody stem tissues identified some metabolites specific to woody stem wounding responses such as naringenin, taxifolin and flavanol gallate accumulation. In this study, we have shown that stilbenes are highly and rapidly accumulated at the graft interface and in response to wounding, and we hypothesise that these stilbenes oligomerize over time. We have also shown that the many other metabolites show large temporal changes in concentration at the graft interface, particularly naringenin and taxifolin. In addition, knowledge of the spatial distribution of metabolites accumulated after wounding or grafting provides insights into their potential roles (summarised in Figure 8). For example, metabolites which accumulate in the damaged xylem parenchyma such as resveratrol could function in plant defence to prevent pathogen infection into perennial woody structures. The hypothesis that resveratrol accumulation at the graft interface is not linked to grafting success is supported by the experiment which showed that exogenous application of resveratrol did not influence grafting success rate. Whereas polyphenols which accumulate in the newly formed callus tissues may have a wider range of roles such as forming new vascular tissues, plant signalling, plant defence and developing a functional graft union.

ACKNOWLEDGEMENTS

We thank Cyril Hevin, Maria Lafargue and Nicolas Hocquard for the grafting plants and Anne Janoueix, Marilou Camboué, Pablo Dupiol and Fernanda Endringer Pinto for helping during the sampling and sample preparation. Research support was provided by the French Ministry of Higher Education, by the European Union INTERREG POCTEFA project Vites Qualitas (EFA 324/19) which is co-financed by the Fonds Européen de Développement Regional (FEDER), and by VitiGraft funded by the Plant2Pro® Carnot Institute in the frame of its 2021 call, Plant2Pro® is supported by ANR (agreement #21-CARN-024-01 – 2021). Some work was done during a short-term scientific mission funded by COST (European Cooperation in Science and Technology) Action CA17111 INTEGRAPE. This work was supported by the Bordeaux Metabolome Facility (https://doi.org/10.15454/1.5572412770331912E12), the MetaboHUB (ANR-11-INBS-0010) project. Support from the Carlsberg Foundation, The Danish Council for Independent Research|Medical Sciences (Grant DFF-4002-00391) for the applied MALDI-MSI instrumentation is gratefully acknowledged.

CONFLICT OF INTEREST STATEMENT

The authors declare no conflict of interest.

DATA AVAILABILITY STATEMENT

All quantification data (means and standard deviation) all conditions studied are given in Supplementary Data S1. HPLC-QqQ data is available on data INRAE (https://doi.org/10.57745/FOLQKK). MALDI-MSI data are available on METASPACE annotations (https://metaspace2020.eu/project/Loupit-2023) (Palmer et al., 2017).

ORCID

Grégoire Loupit http://orcid.org/0000-0002-2411-7428
Josep V. Fonayet http://orcid.org/0000-0002-1359-4114
Christian Janfelt http://orcid.org/0000-0002-4626-3426
Sarah J. Cookson https://orcid.org/0000-0003-2591-192X

REFERENCES

Abbott, E., Hall, D., Hamberger, B. & Bohlmann, J. (2010) Laser microdissection of conifer stem tissues: isolation and analysis of high quality RNA, terpene synthase enzyme activity and terpenoid metabolites from resin ducts and cambial zone tissue of white spruce (*Picea glauca*). *BMC Plant Biology*, 10, 106.

Abreu, I.N., Johansson, A.I., Sokołowska, K., Niittylä, T., Sundberg, B., Hvidsten, T.R. et al. (2020) A metabolite roadmap of the wood-forming tissue in *Populus tremula*. *The New Phytologist*, 228(5), 1559–1572.

An, F., Cui, M., Chen, T., Cheng, C., Liu, Z., Luo, X. et al. (2023) Flavonoid accumulation modulates the responses of cassava tuberous roots to postharvest physiological deterioration. *Postharvest Biology and Technology*, 198, 112254.

Assunção, M., Canas, S., Cruz, S., Brazão, J., Zanol, G.C. & Eiras-Dias, J.E. (2016) Graft compatibility of Vitis spp.: the role of phenolic acids and flavanols. *Scientia Horticulturae*, 207, 140–145.

Assunção, M., Pinheiro, J., Cruz, S., Brazão, J., Queiroz, J., Eiras Dias, J.E. et al. (2019) Gallic acid, sinapic acid and catechin as potential chemical markers of Vitis graft success. *Scientia Horticulturae*, 246, 129–135.

Assunção, M., Santos, C., Brazão, J., Eiras-Dias, J.E. & Fevereiro, P. (2019) Understanding the molecular mechanisms underlying graft success in grapevine. *BMC Plant Biology*, 19(1), 396.

Becker, L., Carré, V., Poutaraud, A., Merdinoglu, D. & Chaimbault, P. (2014) MALDI mass spectrometry imaging for the simultaneous location of resveratrol, pterostilbene and viniferins on grapevine leaves. *Molecules (Basel, Switzerland)*, 19(7), 10587–10600.

Billet, K., Houillé, B., Dugé de Bernonville, T., Besseau, S., Oudin, A., Courdavault, V. et al. (2018) Field-Based metabolomics of *Vitis vinifera* L. stems provides new insights for genotype discrimination and polyphenol metabolism structuring. *Frontiers in Plant Science*, 9, 798.

Bjarnholt, N., Li, B., D'Alvise, J. & Janfelt, C. (2014) Mass spectrometry imaging of plant metabolites—principles and possibilities. *Natural Product Reports*, 31(6), 818–837.

Bokhart, M.T., Nazari, M., Garrard, K.P. & Muddiman, D.C. (2018) MSiReader v1.0: evolving open-source mass spectrometry imaging software for targeted and untargeted analyses. *Journal of the American Society for Mass Spectrometry*, 29(1), 8–16.

Breuil, A.-C., Adrian, M., Pirio, N., Meunier, P., Bessis, R. & Jeandet, P. (1998) Metabolism of stilbene phytoalexins by *Botrytis cinerea*: 1. characterization of a resveratrol dehydrodimer. *Tetrahedron Letters*, 39(7), 537–540.

Canas, S., Assunção, M., Brazão, J., Zanol, G. & Eiras-Dias, J.E. (2015) Phenolic compounds involved in grafting incompatibility of Vitis spp: development and validation of an analytical method for their quantification. *Phytochemical Analysis*, 26(1), 1–7.

Chitarrini, G., Zulini, L., Masuero, D. & Vrhovsek, U. (2017) Lipid, phenol and carotenoid changes in 'Bianca' grapevine leaves after mechanical wounding: a case study. *Protoplasma*, 254(6), 2095–2106.

Chong, J., Poutaraud, A. & Hugueney, P. (2009) Metabolism and roles of stilbenes in plants. *Plant Science*, 177(3), 143–155.

Cookson, S.J., Moreno, M.J.C., Hevin, C., Nyamba Mendome, L.Z., Delrot, S., Trossat-Magnin, C. et al. (2013) Graft union formation in grapevine induces transcriptional changes related to cell wall modification, wounding, hormone signalling, and secondary metabolism. *Journal of Experimental Botany*, 64(10), 2997–3008.

Dardanelli, M.S., Manyani, H., González-Barroso, S., Rodríguez-Carvajal, M.A., Gil-Serrano, A.M., Espuny, M.R. et al. (2010) Effect of the presence of the plant growth promoting rhizobacterium (PGPR) *Chryseobacterium balustinum* Aur9 and salt stress in the pattern of flavonoids exuded by soybean roots. *Plant and Soil*, 328(1–2), 483–493.

DeCooman, L., Everaert, E., Curir, P. & Dolci, M. (1996) The possible role of phenolics in incompatibility expression in *Eucalyptus gunnii* micrografts. *Phytochemical Analysis*, 7, 92–96.

Deng, F., Aoki, M. & Yogo, Y. (2004) Effect of naringenin on the growth and lignin biosynthesis of gramineous plants. *Weed Biology and Management*, 4(1), 49–55.

Errea, P. (1998) Implications of phenolic compounds in graft incompatibility in fruit tree species. *Scientia Horticulturae*, 74, 195–205.

Granborg, J.R., Kaasgaard, S.G. & Janfelt, C. (2022) Mass spectrometry imaging of oligosaccharides following in situ enzymatic treatment of maize kernels. *Carbohydrate Polymers*, 275, 118693.

Hammerbacher, A., Kandasamy, D., Ullah, C., Schmidt, A., Wright, L.P. & Gershenzon, J. (2019) Flavanone-3-hydroxylase plays an important role in the biosynthesis of spruce phenolic defenses against bark beetles and their fungal associates. *Frontiers in Plant Science*, 10, 208.

Hartmann, H.T., Kester, D.E., Davies, Jr. F. & Geneve, R.L. (2011) Plant propagation. Principles and practice. Prentice Hall.

Hu, W., Nie, H., Wang, Y., Li, N., Di, S., Pan, Q. et al. (2022) Tracing the migration and transformation of metabolites in xylem during wood growth by mass spectrometry imaging. *The Analyst*, 147(8), 1551–1558.

Hudina, M., Orazem, P., Jakopic, J. & Stampar, F. (2014) The phenolic content and its involvement in the graft incompatibility process of various pear rootstocks (*Pyrus communis* L.). *Journal of Plant Physiology*, 171(5), 76–84.

Kawamoto, T. (2003) Use of a new adhesive film for the preparation of multi-purpose fresh-frozen sections from hard tissues, whole-animals, insects and plants. *Archives of Histology and Cytology*, 66(2), 123–143.

Khattab, I.M., Sahi, V.P., Baltenweck, R., Maia-Grondard, A., Hugueney, P., Bieler, E. et al. (2021) Ancestral chemotypes of cultivated grapevine with resistance to Botryosphaeriaceae-related dieback allocate metabolism towards bioactive stilbenes. *The New Phytologist*, 229(2), 1133–1146.

El Khawand, T., Gabaston, J., Taillis, D., Iglesias, M.-L., Pedrot, E., Palos Pinto, A. et al. (2020) A dimeric stilbene extract produced by oxidative coupling of resveratrol active against *Plasmopara viticola* and *Botrytis cinerea* for vine treatments. *OENO One*, 54(1), 157–164.

Londo, J.P. & Johnson, L.M. (2014) Variation in the chilling requirement and budburst rate of wild Vitis species. *Environmental and Experimental Botany*, 106, 138–147.

Loupit, G. & Cookson, S.J. (2020) Identifying molecular markers of successful graft union formation and compatibility. *Frontiers in Plant Science*, 11, 610352.

Loupit, G., Fonayet, J.V., Prigent, S., Prodhomme, D., Spilmont, A.-S., Hilbert, G. et al. (2022) Identifying early metabolite markers of successful graft union formation in grapevine. *Horticulture Research*, 9, uhab070.

Loupit, G., Prigent, S., Franc, C., Revel, G., de Richard, T., Cookson, S.J. et al. (2020) Polyphenol profiles of just pruned grapevine canes from wild vitis accessions and *Vitis vinifera* cultivars. *Journal of Agricultural and Food Chemistry*, 68(47), 13397–13407.

Maia, M., McCann, A., Malherbe, C., Far, J., Cunha, J., Eiras-Dias, J. et al. (2022) Grapevine leaf MALDI-MS imaging reveals the localisation of a putatively identified sucrose metabolite associated to *Plasmopara viticola* development. *Frontiers in Plant Science*, 13, 1012636.

Melnyk, C.W. (2017) Plant grafting: insights into tissue regeneration. *Regeneration (Oxford, England)*, 4(1), 3–14.

Morris, H., Hietala, A.M., Jansen, S., Ribera, J., Rosner, S., Salmeia, K.A. et al. (2020) Using the CODIT model to explain secondary metabolites of xylem in defence systems of temperate trees against decay fungi. *Annals of Botany*, 125(5), 701–720.

Mudge, K., Janick, J., Scofield, S. & Goldschmidt, E.E. (2009) A history of grafting. In: Janick, J. (Ed.) *Horticultural reviews*. John Wiley & Sons, Inc, pp. 437–493.

Musacchi, S., Pagliuca, G., Maddalena, K., Piretti, M.V. & Sansavini, S. (2000) Flavonoids as markers for Pear-quince graft incompatibility. *Journal of Applied Botany*, 74, 206–211.

Noronha, H., Garcia, V., Silva, A., Delrot, S., Gallusci, P. & Gerós, H. (2021) Molecular reprogramming in grapevine woody tissues at bud burst. *Plant Science: An International Journal of Experimental Plant Biology*, 311, 110984.

Notaguchi, M., Kurotani, K.-I., Sato, Y., Tabata, R., Kawakatsu, Y., Okayasu, K. et al. (2020) Cell-cell adhesion in plant grafting is facilitated by β-1,4-glucanases. *Science (New York, N.Y.)*, 369(6504), 698–702.

Ollat, N., Peccoux, A., Papura, D., Esmenjaud, D., Marguerit, E., Tandonnet, J.-P. et al. (2015) Rootstocks as a component of adaptation to environment. In: Gerós, H., Chaves, M.M., Gil, H.M., Delrot, S. (Eds.) *Grapevine in a Changing Environment*. John Wiley & Sons, Ltd. pp. 68–108.

Ozfidan-Konakci, C., Yildiztugay, E., Alp, F.N., Kucukoduk, M. & Turkan, I. (2020) Naringenin induces tolerance to salt/osmotic stress through the regulation of nitrogen metabolism, cellular redox and ROS scavenging capacity in bean plants. *Plant Physiology and Biochemistry*, 157, 264–275.

Palmer, A., Phapale, P., Chernyavsky, I., Lavigne, R., Fay, D., Tarasov, A. et al. (2017) FDR-controlled metabolite annotation for high-resolution imaging mass spectrometry. *Nature Methods*, 14(1), 57–60.

Papastamoulis, Y., Bisson, J., Temsamani, H., Richard, T., Marchal, A., Mérillon, J.-M. et al. (2015) New E-miyabenol isomer isolated from grapevine cane using centrifugal partition chromatography guided by mass spectrometry. *Tetrahedron*, 71(20), 3138–3142.

Pawlus, A.D., Sahli, R., Bisson, J., Rivière, C., Delaunay, J.-C., Richard, T. et al. (2013) Stilbenoid profiles of canes from vitis and Muscadinia species. *Journal of Agricultural and Food Chemistry*, 61(3), 501–511.

Pl@ntGrape Database. (2009) *Catalogue des vignes cultivées en France, IFV —INRAE—l'Institut Agro Montpellier SupAgro 2009-2020*.

Prodhomme, D., Valls Fonayet, J., Hévin, C., Franc, C., Hilbert, G. & Revel, G. et al. (2019) Metabolite profiling during graft union formation reveals the reprogramming of primary metabolism and the induction of stilbene synthesis at the graft interface in grapevine. *BMC Plant Biology*, 19(1), 599.

Rice-Evans, C. (1995) Plant polyphenols: free radical scavengers or chain-breaking antioxidants? *Biochemical Society Symposia*, 61, 103–116.

Robichaud, G., Garrard, K.P., Barry, J.A. & Muddiman, D.C. (2013) MSiReader: an open-source interface to view and analyze high resolving power MS imaging files on Matlab platform. *Journal of the American Society for Mass Spectrometry*, 24(5), 718–721.

Rouphael, Y., Schwarz, D., Krumbein, A. & Colla, G. (2010) Impact of grafting on product quality of fruit vegetables. *Scientia Horticulturae*, 127(2), 172–179.

Santos Wagner, A.L., Araniti, F., Ishii-Iwamoto, E.L. & Abenavoli, M.R. (2022) Resveratrol exerts beneficial effects on the growth and metabolism of *Lactuca sativa* L. *Plant Physiology and Biochemistry*, 171, 26–37.

Seigler, D.S. (2006) Basic pathways for the origin of allelopathic compounds. In: Reigosa, M.J., Pedrol, N. & González, L. (Eds.) *Allelopathy*. Kluwer Academic Publishers. pp. 11–61.

Słupianek, A., Dolzblasz, A. & Sokołowska, K. (2021) Xylem Parenchyma-Role and relevance in wood functioning in trees. *Plants (Basel, Switzerland)*, 10(6), 1247.

Usenik, V., Krška, B., Vičan, M. & Štampar, F. (2006) Early detection of graft incompatibility in apricot (*Prunus armeniaca* L.) using phenol analyses. *Scientia Horticulturae*, 109(4), 332–338.

Vega-Muñoz, I., Duran-Flores, D., Fernández-Fernández, Á.D., Heyman, J., Ritter, A. & Stael, S. (2020) Breaking bad news: dynamic molecular mechanisms of wound response in plants. *Frontiers in Plant Science*, 11, 610445.

Volf, I., Toma, I., Toma, C., Popescu, M.G. & Popa, V.I. (2006) Aromatic compounds from wood as regulating agents for grafting processes. *Cellulose Chemistry and Technology*, 40, 13–18.

Wilkens, A., Paulsen, J., Wray, V. & Winterhalter, P. (2010) Structures of two novel trimeric stilbenes obtained by horseradish peroxidase catalyzed biotransformation of trans-resveratrol and (-)-epsilon-viniferin. *Journal of Agricultural and Food Chemistry*, 58(11), 6754–6761.

Yang, G., Liang, K., Zhou, Z., Wang, X. & Huang, G. (2020) UPLC-ESI-MS/MS-Based widely targeted metabolomics analysis of wood metabolites in teak (*Tectona grandis*). *Molecules (Basel, Switzerland)*, 25(9), 2189.

Yang, L., Wen, K.-S., Ruan, X., Zhao, Y.-X., Wei, F. & Wang, Q. (2018) Response of plant secondary metabolites to environmental factors. *Molecules (Basel, Switzerland)*, 23(4), 762.

Yildiztugay, E., Ozfidan-Konakci, C., Kucukoduk, M. & Turkan, I. (2020) Flavonoid naringenin alleviates short-term osmotic and salinity stresses through regulating photosynthetic machinery and chloroplastic antioxidant metabolism in *Phaseolus vulgaris*. *Frontiers in Plant Science*, 11, 682.

Yoshinaga, A., Kamitakahara, H. & Takabe, K. (2016) Distribution of coniferin in differentiating normal and compression woods using MALDI mass spectrometric imaging coupled with osmium tetroxide vapor treatment. *Tree Physiology*, 36(5), 643–652.

SUPPORTING INFORMATION

Additional supporting information can be found online in the Supporting Information section at the end of this article.

How to cite this article: Loupit, G., Fonayet, J.V., Lorensen, M.D.B.B., Franc, C., De Revel, G., Janfelt, C. et al. (2023) Tissue-specific stilbene accumulation is an early response to wounding/grafting as revealed by using spatial and temporal metabolomics. *Plant, Cell & Environment*, 46, 3871–3886. https://doi.org/10.1111/pce.14693